The Luminosity function of Macronovae

Stefano Ascenzi[1 2 3] Ryan Foley[4] Enrico Ramirez-Ruiz[3 4]
Stephan Rosswog[5] Brenna Mockler[4]
Ariadna Murguia-Berthier[4] Chris Fryer[6 7]
Nicole Lloyd-Ronning[7] Silvia Piranomonte[8]

[1] *Dip. di Fisica, Universita' di Roma La Sapienza, P.le A. Moro, 2, I-00185 Rome, Italy*
[2] *Università di Roma Tor Vergata, Via della Ricerca Scientifica 1, I-00133 Roma, Italy*
[3] *DARK, Niels Bohr Institute, University of Copenhagen, Blegdamsvej 17, 2100 Copenhagen, Denmark*
[4] *Department of Astronomy and Astrophysics, University of California, Santa Cruz, CA 95064, USA*
[5] *The Oskar Klein Centre, Department of Astronomy, AlbaNova, Stockholm University, SE-106 91 Stockholm, Sweden*
[6] *Department of Physics, The University of Arizona, Tucson, AZ 85721, USA*
[7] *Center for Theoretical Astrophysics, Los Alamos National Lab, Los Alamos, NM 87544, USA*
[8] *INAF - Osservatorio Astronomico di Roma, Monte Porzio Catone (RM), Italy*

Abstract

The coalescence of compact binary systems composed by neutron stars (NS) and black holes (BH) is one of the principal source of gravitational waves (GW) in the LIGO and Virgo frequency range. While BH binary mergers are not expected to generate any electromagnetic signature, binary NS and NS-BH mergers could be followed by detectable electromagnetic counterparts. Observinging both gravitational and electromagnetic signals is important because it is possible to obtain complementary informations about the source from these two different messengers. For example a GW detection could provide the masses and the spins of the compact objects, while electromagnetic emission is essential for the source localization, which enables the identification of the host galaxy.

Among all the possible electromagnetic counterparts of binary NS and NS-BH mergers Macronovae (or Kilonovae) play a special role because they are isotropic, therefore they could be observed after every binary NS (and some NS-BH) merger detected by GW interferometers. Marconovae are hypothetical optical-near infrared (NIR) transients powered by radioactive decay of r-process elements synthesized within neutron rich matter ejected during the merger. Macronovae have not been unambiguously detected so far,

however three candidates have been observed after short gamma ray bursts (GRB). In this work we want to use these three events along with GRBs without a related macronova candidate to constrain the luminosity function of macronovae, which is a fundamental tool for the astronomers to plan an observational strategy in order to detect for the first time these unique astrophysical transients.

1 Introduction

The direct observation of the first GW by the two terrestrial interferometers LIGO, GW150914 [Abbott et al., 2016a], marked the down of a new era of astronomy: the GW astronomy era. After the first detection two more events have been discovered by LIGO: GW151226 [Abbott et al., 2016b] and GW170104 [Abbott et al., 2017] along with the candidate event LVT151012, which has a probability of being of astrophysical origin of 87% [Abbott et al., 2016c]. All these GW signals were compatible with waveforms predicted for mergers of two BHs in a binary system.

The 1st of August 2017 the European interferometer Virgo joined LIGO in the observation and on the 14th of August a network of three detectors observed its first GW event: GW170814 [The LIGO Scientific Collaboration et al., 2017]. Even in this case the origin of the signal was a BH binary coalescence. The presence of a third observing detector it is fundamental because it allows a better constrain on the spatial origin of the GW source, improving its sky localization to an area of $O(10-100\,deg^2)$ from an area of $O(100-1000\,deg^2)$ with only two interferometers. To constrain the sky position of the source is fundamental, because it allows astronomers to find a possible related electromagnetic counterpart of the GW signal. The identification of an electromagnetic counterpart is very important not only because it could give us complementary informations about the source (like for example magnetic field and matter properties) with respect to those provided by GW, but also because allows a more precise localization (within arcseconds) of the source in the sky, which could lead to the host galaxy identification and thus the redshift determination.

However BH binary coalescences are not expected to produce any electromagnetic counterpart, at least in those cases where the merger takes place in a gas poor environment. In order to radiate photons a compact binary merger in the LIGO-Virgo frequency range should be composed at least by one NS.

During a binary NS or a NS-BH merger a NS could be tidally disrupted and a fraction of its matter expelled from the system on a dynamical timescale (in the case of NS-BH merger it can happen only for a small range of parameters as shown for example in Pannarale and Ohme [2014]). In a binary NS coalescence matter could be also ejected at the same timescales due to the squeezing in the interface

between the two merging stars [Rosswog et al., 2017]. These matter components ejected on dynamical timescales are called in general *dynamical ejecta*. Since the dynamical ejecta is composed by the matter of the former NS its electron fraction ($Y_e \equiv n_e/(n_e+n_n)$, where n_e and n_n is the number density of electrons and neutrons) is very low ($Y_e < 0.3$), which means that the matter is highly neutron rich. Such an environment is the perfect site for r-process nucleosynthesis, where the nuclides in the dynamical ejecta capture free neutrons on a characteristic timescale that is shorter than the timescale of β-decay. In this way the heaviest elements in the universe, Lanthanides and Actinides among them, are synthesized.

Once the neutron rich and unstable nuclei decay they emit γ-rays, β and α-particles and fission fragments, which thermalize efficiently and inject energy in the surroundings [Barnes et al., 2016]. This energy injection could in principle power an electromagnetic transient, known as *kilonova* or *macronova* [Li and Paczyński, 1998].

This report is organized as follows: in Section 2 will be presented a toy macronova model in order to introduce the main parameters that influence the macronova emission features. Moreover two fitting formulas to express the velocity and the mass of dynamical ejecta as a function of the initial binary system mass ratio will be presented. In Section 3 will be exposed the goal of the present work and the methodology that will be applied to reach it. In Section 4 the conclusions obtained so far will be summarized and there will be a description of the next steps of the project.

2 Macronova Parameters

The most important parameters that determine the features of the macronova emission are three: the opacity k of the matter, the mass of the ejecta m_{ej} and the ejecta velocity v_{ej}. It is possible to show how these parameters affect the emission with the aid of a toy model: consider the dynamical ejecta as a spherical cloud of matter with mass m_{ej} and opacity k, expanding with velocity v_{ej}. The optical depth τ of the cloud is:

$$\tau = \rho k R = \frac{3 k m_{ej}}{4\pi R^2} \tag{1}$$

where we expressed the density as the average density inside the cloud. From this expression we can calculate the diffusion timescale within the ejecta:

$$t_{diff} = \frac{R}{c}\tau = \frac{3 k m_{ej}}{4\pi c R} = \frac{3 k m_{ej}}{4\pi c v_{ej} t} \tag{2}$$

where we expressed the expansion radius R as the velocity of the ejecta times the expansion timescale t. The peak of the emission takes place when the expansion

and the diffusion timescales become equal, since the bulk of the photons are able to leave the nebula. Hence, solving the equation $t_{diff}(t) = t$ the time of the peak can be obtained [Arnett, 1982]:

$$t_{peak} = \sqrt{\frac{3km_{ej}}{4\pi c v_{ej}}} \tag{3}$$

It is possible to calculate the peak luminosity in a similar fashion. Since the source of macronova emission is the radioactive decay of newly r-process synthesized elements at each times the bolometric luminosity can be expressed in the following way:

$$L(t) = \dot{\varepsilon}(t) m_{ej} \tag{4}$$

where $\dot{\varepsilon}(t)$ is the heating rate per unit mass. The heating rate is assumed to be constant as long as the neutron capture is proceeding (until 1 second after the merger) and drops later as a power law of index $\alpha \simeq 1.3$. This behavior is motivated by the fact that this power law roughly corresponds to the superimposition of the exponential decays of all isotopes that compose the ejecta [Metzger et al., 2010], [Roberts et al., 2011], [Korobkin et al., 2012], [Hotokezaka et al., 2016]. Since the peak occurs much later than 1 second after the merger we are in the power low regime and the peak luminosity can be expressed as:

$$L_{peak} = \dot{\varepsilon}_0 \Big(\frac{t_{peak}}{t_0}\Big)^{-1.3} m_{ej} = \dot{\varepsilon}_0 \Big(\frac{3k}{4\pi c v_{ej} t_0^2}\Big)^{-0.65} m_{ej}^{0.35} \tag{5}$$

where $\dot{\varepsilon}_0$ and t_0 are the heating rate and the time at the onset of power law trend.

From equations 3 and 5 it is possible to notice that increasing the opacity the energy emission is spread on longer timescales, resulting thus in a fainter transient that peaks later in time. In a similar fashion decreasing the velocity cause an increase of diffusion timescale, which results once again in lower luminosity and higher t_{peak}. A different trend is observed when mass is increased, because t_{peak} became higher and so does the peak luminosity, since more radioactive fuel is provided. The opacity is not only affected by the composition of the ejecta, but also by the method we choose to calculate it (see Kasen et al. [2015] and Fontes et al. [2017] for two different treatment of the opacity within an expanding medium).

The mass and velocity of the ejecta are determined by the dynamic of binary neutron star merger and one may wonder if those parameters are truly independent or they are somehow correlated. In Figure 1 we plotted on $v_{ej} - m_{ej}$ parameter space the mass and velocity obtained by a set of smoothed particle hydrodynamic (SPH) numerical simulations [Korobkin et al., 2012] as well as the parameters used in Barnes & Kasen and Los Alamos group macronova models. The mass

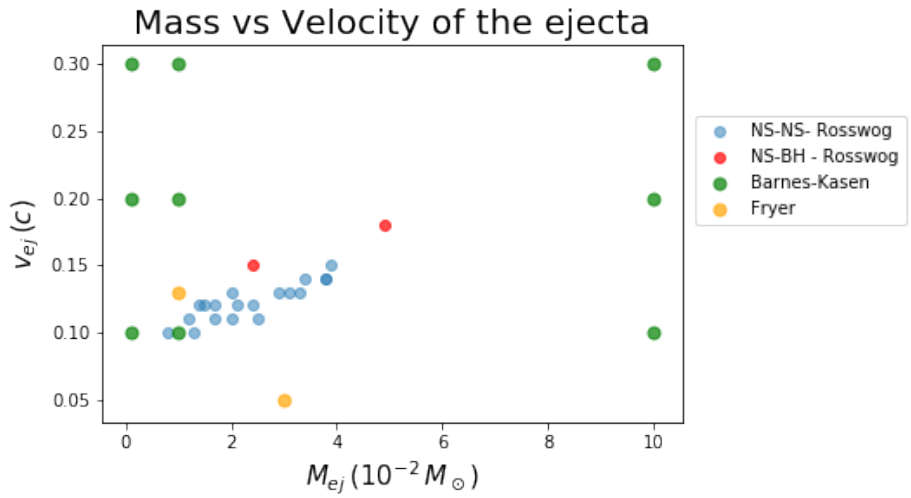

Figure 1: Dynamical ejecta mass and velocity parameter space. The green and the yellow dots represent the parameters explored in Barnes & Kasen [Barnes and Kasen, 2013] and Los Alamos group [Wollaeger et al., 2017] macronova models respectively. Blue and red dots represent respectivelly the outcomes of SPH numerical simulations of NS-NS and NS-BH mergers [Korobkin et al., 2012].

and velocity that results from numerical simulation are clearly correlated, which means that, given the opacity, macronova emission can be described by just one parameter. We choose the mass ratio of the binary system to parametrize the mass and the the velocity of the ejecta and we define the mass ratio as $q = m_2/m_1$, where m_2 and m_1 are the masses of the lighter and havier component respectively.

In order to express the ejecta mass as a function of q we used the Korobkin equation [Korobkin et al., 2012], a formula whose parameters are obtained fitting results of the same SPH simulations shown in Figure 1:

$$m_{ej}(q, M_{tot}) = M_{tot} * \left(A - B\eta(q) - \frac{C}{1+\eta^3(q)/\sigma^3}\right) \tag{6}$$
$$\eta(q) = \eta(1/q) = 1 - 4\frac{q}{(1+q)^2}$$

with $A = 0.0125$, $B = 0.015$, $C = 0.0083$ and $\sigma = 0.0056$.

The velocity of the ejecta instead scales linearly with the mass ratio q in agreement with the equation:

$$v(q) = D_2 q + D_1 \tag{7}$$

Performing a linear fit of the simulation data we find the intercept and angular

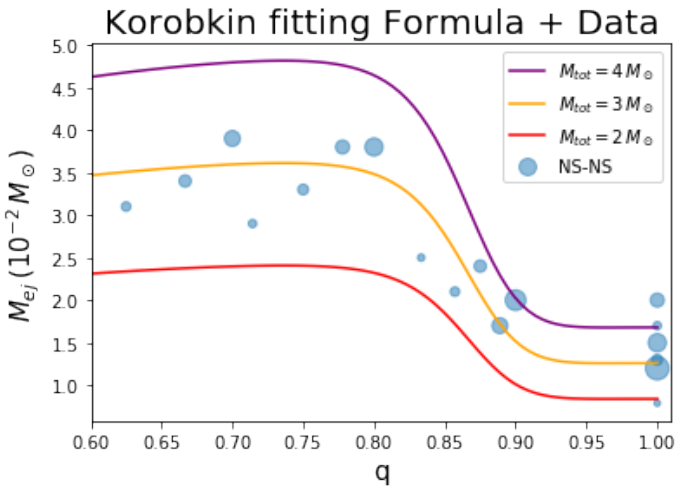

Figure 2: Korobkin formula (equation 6) for binary system total mass equal to $2M_\odot$,$3M_\odot$ and $4M_\odot$ as a function of the mass ratio q. Blue dots represents results of simulations, where the area of the dots increases with higher initial total mass of the binary system.

coefficient with values $D_1 = 0.199$ and $D_2 = -0.089$ respectively.

In Figure 2 and 3 the fitting formulas are plotted with the data points. The area of the points scales with the total mass of the binary system and it is worth noticing that not only the mass ratio but also the total mass determines the final ejecta mass and velocity outcome (as also suggested by equation 6). Nevertheless this dependence is rather weak in comparison with the q dependence so we can neglect it as a first approximation.

3 Methodology

In order to find the luminosity function of macronovae we need to know how the parameters that determine the features (*i.e.* peak luminosity, time of the peak) of macronova emission are distribuited. Once the parameter distributions are obtained it is possible to calculate the luminosity function, which can be defined, for example, as the distribution of the peak luminosities or the the luminosities at certain amount of days after the merger.

As it was already stated in the previous section, given a matter composition and once an opacity prescription is chosen, the two parameters that mainly determine the features of macronova emission are m_{ej} and v_{ej}. Since ejecta mass and

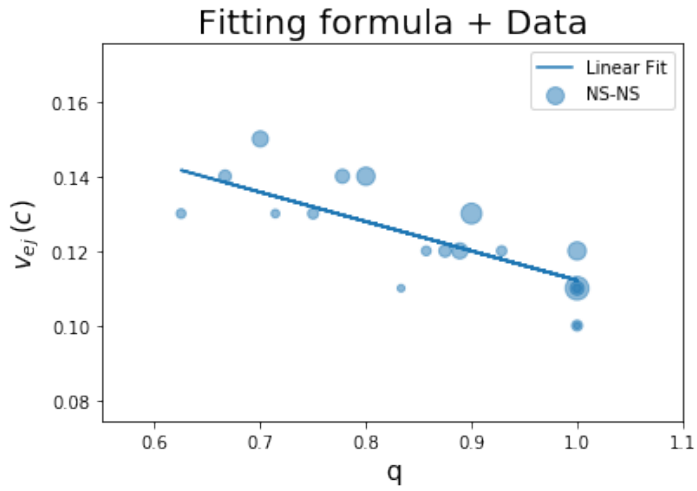

Figure 3: Linear fit of ejecta velocity with data from simulations. The area of the dots increases with higher initial total mass of the binary system.

velocity can be parametrized by the mass ratio q, the problem of finding the luminosity function of macronovae can be recast in finding the mass ratio distribution of macronovae progenitors.

In order to attempt this goal we are using MOSFiT, a code that uses a Monte Carlo Markov Chain (MCMC) method to fit light curves of transients. We consider a set of 15 GRB afterglows, three of which (GRB050709, GRB060614 and GRB130603B) present a late time excess in the NIR. Although these excesses are only observed as single photometric points, so far they costitute the best macronova candidates that we have. If we consider these macronova candidates as actual macronovae we can use MOSFiT to fit the afterglow datas with afterglow+macronova models in order to obtain a distribution for the mass ratio q. In the analysis all the afterglows without late time excess will provide an upper limit on the macronova emission, which corresponds to a lower limit on q.

3.1 MOSFiT

MOSFiT (Modular Open Source Fitter for Transients) is a Python based code to fit lightcurves of transients and estimate the parameters distribution given a user defined model. The structure and the usage of the code are described in Guillochon et al. (in preparation), while in Nicholl et al. [2017] some of the main features are summarized. The code takes in input a model file, which contains a chain of Python modules describing the physics of the problem and a parameter file, which

lists the parameters used and their range. These file are needed to produce module multicolor light curves that have to be fitted with the observed data. The fitting is done using a MCMC fitter that maximize the following log likelihood:

$$\ln \mathscr{L} = -\frac{n}{2}\ln(2\pi\sigma^2) - \frac{1}{2}\sum_{i=1}^{n}\Big[\frac{(O_i - M_i)^2}{\sigma_i^2 + \sigma^2} - \ln(2\pi\sigma_i^2)\Big] \tag{8}$$

where O_i and M_i are the observed and model magnitudes, σ_i is the observed error and σ is a modeled white noise error term.

In our analysis we use mainly two different MOSFiT modules to produce the afterglow multicolor light curves: the engine and the spectral energy distribution (SED).

The engine module provide the bolometric light curve of the transient, which is described in the case of a GRB afterglow as a broken power law:

$$L(t_d) = \begin{cases} L_{1d} t_d^{-\alpha_1} & t_d \leq t_{break} \\ \\ L_{1d} t_{break}^{\alpha_2 - \alpha_1} t_d^{-\alpha_2} & t_{break} \leq t_d \end{cases} \tag{9}$$

where t_d is the time measured in days, α_1 and α_2 are the two power law indices, with $\alpha_1 \leq \alpha_2$, t_{break} is time of the break and L_{1d} is the luminosity one day after the GRB prompt emission.

The SED module takes the bolometric luminosity in input and use a user defined SED to distribute the energy among the different frequencies in order to produce multicolor lightcurves.

Although the afterglow spectrum is well described by a broken power law with three break frequencies [Sari et al., 1998], as a first guess we described it with a simple power law, do to the fact that we are using data in the optical-NIR band and it is unlikely that a break frequency fall within such a small frequency range:

$$F(t_d, \nu) \propto L(t_d)\nu^{-\beta}. \tag{10}$$

After the SED module the photometry module it is used to redshift the SED and convolve it with filter functions for each observed band, while the extinction module correct for the extinction of the Milky Way and the host galaxy.

For our problem we need to superimpose a macronova to the afterglow model. Although MOSFiT is already provided by a built-in macronova model it is a semi-analytic model and takes ejecta mass and velocity as input parameters. Instead we intend to exploit of the Barnes & Kasen models that are obtained from a detailed radiative transfer calculation [Barnes and Kasen, 2013]. Since in this case the SEDs are already provided we intend to simply insert them in the SED module without

passing through the engine module. In order to attempt this goal it is required an interpolation between the macronova models. All the details of the interpolation will be discussed in section 3.3.

3.2 Dataset

In this section the sample of GRBs as well as the theoretical macronova model used in our analysis will be described.

3.2.1 GRB sample

Our GRB sample is comprised by 15 GRBs, all of them with observed optical afterglow and 3 of whom (GRB050709, GRB060614 and GRB130603B) show a NIR excess as a single photometric point compatible with a macronova emission [Tanvir et al., 2013], [Berger et al., 2013], [Yang et al., 2015], [Jin et al., 2016]. All the SGRB in the sample are reported in Fong et al. [2015] except GRB060614 that, although shares many properties with short duration GRB (temporal lag, peak luminosity, host galaxy and lack of coincident supernova), has the duration of a long GRB (102 s). In Table 1 the redshift z and the T_{90} duration (the time over which a GRB emits from 5% to 95% of its total measured counts [Koshut et al., 1995]) of the GRBs in the samples are listed.

3.2.2 Macronova Models

Macronova models that have been used are those reported in Barnes and Kasen [2013]. In these models a spherical ejecta morphology is considered, with a density profile scaling with the distance r from the centre as a broken power law. The opacity of the expanding ejecta have been calculated using the Sobolev formalism [Sobolev, 1960], which requires that the width of the lines is small with respect to the characteristic scale of matter properties variation (such that the matter properties can be considered constant over the line resonance region) and that there is no superimposition among the lines (see Fontes et al. [2017] and Wollaeger et al. [2017] for an alternative approach). Also local thermodynamic equilibrium is considered, which is a valid approximation as far as the ejecta is in the optically thick regime, until about one week after the merger. The composition of the matter taken into account is a mixture of Calcium (Ca), Iron (Fe) and Neodymium (Nd), where the latter represents all the lanthanides.

As regards the ejecta dynamical properties the authors considered masses of 0.001, 0.01 and $0.1\,M_{\odot}$ and velocities of 0.1, 0.2 and $0.3\,c$ and obtained a spectrum for all their combinations. The nine resultant model in the parameter space are represented by green dots in Figure 1.

GRB	$T_{90}(s)$	z
050709*	0.07	0.161
050724A	3.0	0.257
051221A	1.4	0.546
060121	2.0	<4.1
060313	0.7	<1.7
060614*	102	0.125
070707	1.1	<1.1
080503	0.3	<3.6
090305A	0.4	<4.1
090426	1.3	2.609
090510	0.3	0.903
130603B*	0.18	0.356
130912A	0.28	<4.1
140903A	0.30	0.351
150101B	0.018	0.134

Table 1: List of GRBs in the sample with their T_{90} duration in seconds and the redshift z. The * denotes those GRBs with a NIR excess.

Model	$v_{ej}(c)$	$m_{ej}(M_{\odot})$
bp_CaFN_hv_h	0.3	0.1
bp_CaFN_hv_m	0.3	0.01
bp_CaFN_hv_l	0.3	0.001
bp_CaFN_mv_h	0.2	0.1
bp_CaFN_mv_m	0.2	0.01
bp_CaFN_mv_l	0.2	0.001
bp_CaFN_lv_h	0.1	0.1
bp_CaFN_lv_m	0.1	0.01
bp_CaFN_lv_l	0.1	0.001

Table 2: List of macronova models from Barnes and Kasen [2013] with mass and velocity of ejecta.

3.3 Interpolation

In order to be used by MOSFiT our models must be described by a set of continuous parameters. Instead we have nine different macronova SEDs for nine different ejecta mass and velocity pairs. Moreover we can see in Figure 1 that most of these pairs of parameters explored by macronova models are non-physical because they do not follow the correlation highlighted by numerical simulations.

In order to obtained a continuos coverage of the parameter space we performed a linear interpolation of our set of models (the nine Barnes & Kasen models) in the mass and velocity plane. For the linear interpolation we used the *interpolate.griddata* tool of *SciPy* Python library that first tassellates the input set of data points with triangles (or n-dimensional simplicities if $n > 2$) and then interpolate on each triangle. In our case the data points are the specific fluxes (in μJy) at the nine different points in mass and velocity parameter space considered at a fixed time and a fixed frequency. The result of the interpolation projected in mass-flux and velocity-flux plane is represented respectively in Figure 4 and Figure 5, where the flux is calculated at time $t = 12960\,s$ at frequency $\nu = 6.85 \times 10^{14}\,Hz$.

The interpolation is then repeated for each time and each frequency in order to obtain for each point on the parameter space a set of spectra (one spectrum per different time).

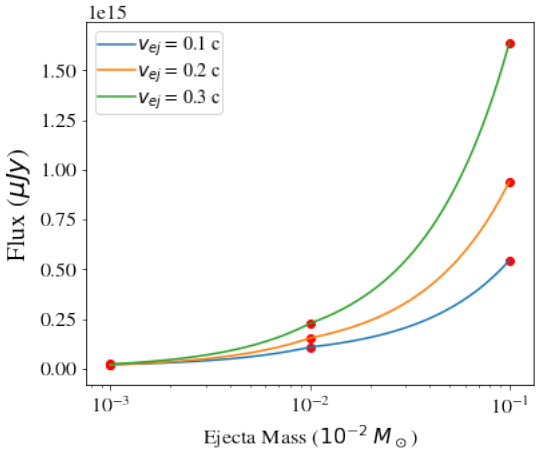

Figure 4: Result of the linear interpolation projected in the mass-flux plane. The red dots represent the flux of the nine macronova models at time $t = 12960\,s$ and frequency $\nu = 6.85 \times 10^{14}\,Hz$ while the curves represent the interpolation at three different value of the ejecta velocity.

Once a dense coverage of the parameter space had been obtained the next step

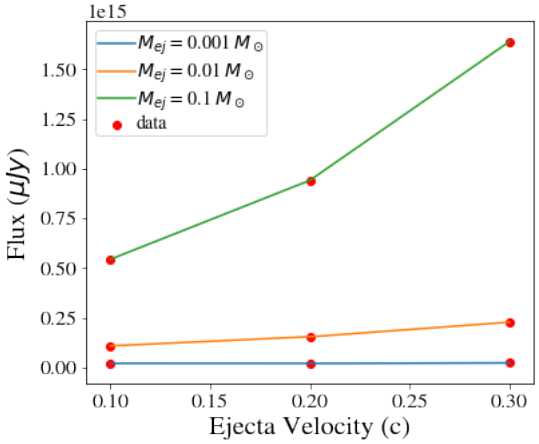

Figure 5: Result of the linear interpolation projected in the velocity-flux plane. The curves represent the interpolation at three different values of the ejecta mass.

was to select only the physical models, namely those generated from a mass and velocity pair that satisfies the correlation highlighted by numerical simulations. In order to reach this goal we used equations 6 and 7 to define a curve on the mass and velocity space parametrized by the mass ratio q. The physical model are only those described by parameters laying on the curve; in this way for any given mass ratio q it is possible to recover a macronova spectrum at each time. We show in Figure 6 how at different times the flux obtained from the interpolation change with the mass ratio. Here the flux is calculated at the fixed frequency $\nu = 1.35 \times 10^{14}$ Hz, which is close to the peak emission frequency. We can see that about 5 days after the merger the flux roughly double moving from $q = 1$ to $q = 0.6$.

Figure 7 instead show the entire spectra obtained by our interpolation for different mass ratio q.

It is worth noticing that we limited our analysis to mass ratios in the range $[0.6, 1]$, which is a reasonable range for NS-NS merger. NS-BH merger would require lower mass ratios along with different mass and velocity fitting formulas, but we did not include this case in the analysis.

4 Conclusions

In these conclusive remarks I summarize the procedure we intend to use in order to find the luminosity function of macronovae and I will show some preliminary results that I am still improving. Then I will describe the next steps to reach the

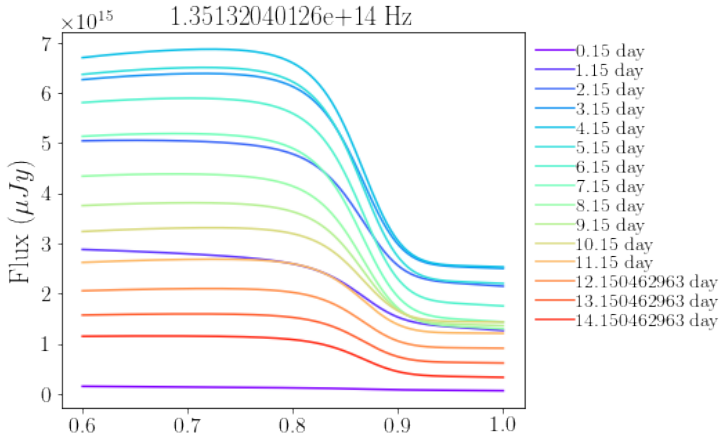

Figure 6: Flux at the frequency $\nu = 1.35 \times 10^{14}$ Hz as a function of the mass ratio q at different times after the merger.

final goal of the project.

We intend to obtain the luminosity function of macronovae starting from the probability distribution of parameters that determine the macronova emission features. These parameters are the mass and the velocity of the dynamical ejecta. However SPH numerical simulations show that they are not independent parameters but they are instead correlated. This evidence allows us to use a single parameter to describe macronova models and we find that the best parameter is the mass ratio q of the initial binary system. We interpolate in the ejecta mass and velocity space the nine macronova models reported in Barnes and Kasen [2013] in order to obtain a dense coverage on the parameter space, then we select those models that lies on a "physical" trajectory parametrized by the mass ratio q defined by equations 6 and 7. The models selected in this way are those that describe a macronova that could occur in nature, according to our current knowledge of the binary NS merger physics.

A problem that has not be accounted in our analysis is the treatment of the opacity. In Figure 8 it is shown a comparison at about 1 day after the merger between two Barnes & Kasen spectra (bp_CaFN_lv_l and bp_CaFN_lv_m in Table 2) and a spectrum from the Los Alamos group (the SAd model in Wollaeger et al. [2017]) characterized by $m_{ej} = 0.014 M_{\odot}$ and $v_{ej} = 0.125 c$. The latter model differs from the former ones by the treatment of the opacity, which is not calculated by Sobolev approximation but with a line-smeared approach presented in Fontes et al. [2017] that preserve the integral of the opacity over frequency. From the figure we can see that the opacity treatment has an important impact on the spec-

trum, since the Wollaeger spectrum, whose parameters are close to those of model bp_CaFN_lv_m, departs significantly for it and crosses both bp_CaFN_lv_l and bp_CaFN_lv_m models. This difference in the spectra is relevant and tells us that our analysis will be necessarily model dependent.

The work is still in progress. In Figure 9 I show one of my first attempt to use MOSFiT to fit the afterglow model described in Section 3.1 on the data of GRB 060121, which is a short GRB that shows no NIR excess. A longer run is needed as well as a refinement of the afterglow model (the condition $\alpha_1 \leq \alpha_2$ for the power indices of the bolometric lightcurve must be imposed) in order to improve the fit. The next step will be to provide MOSFiT the macronova model I obtained from the interpolation and use the code to constrain the mass ratio distribution, which will be used to obtain the luminosity function of macronovae.

References

B. P. Abbott, R. Abbott, T. D. Abbott, M. R. Abernathy, F. Acernese, K. Ackley, C. Adams, T. Adams, P. Addesso, R. X. Adhikari, and et al. Observation of Gravitational Waves from a Binary Black Hole Merger. *Physical Review Letters*, 116(6):061102, February 2016a. doi: 10.1103/PhysRevLett.116.061102.

B. P. Abbott, R. Abbott, T. D. Abbott, M. R. Abernathy, F. Acernese, K. Ackley, C. Adams, T. Adams, P. Addesso, R. X. Adhikari, and et al. GW151226: Observation of Gravitational Waves from a 22-Solar-Mass Binary Black Hole Coalescence. *Physical Review Letters*, 116(24):241103, June 2016b. doi: 10.1103/PhysRevLett.116.241103.

B. P. Abbott, R. Abbott, T. D. Abbott, M. R. Abernathy, F. Acernese, K. Ackley, C. Adams, T. Adams, P. Addesso, R. X. Adhikari, and et al. Binary Black Hole Mergers in the First Advanced LIGO Observing Run. *Physical Review X*, 6(4): 041015, October 2016c. doi: 10.1103/PhysRevX.6.041015.

B. P. Abbott, R. Abbott, T. D. Abbott, F. Acernese, K. Ackley, C. Adams, T. Adams, P. Addesso, R. X. Adhikari, V. B. Adya, and et al. GW170104: Observation of a 50-Solar-Mass Binary Black Hole Coalescence at Redshift 0.2. *Physical Review Letters*, 118(22):221101, June 2017. doi: 10.1103/PhysRevLett.118.221101.

W. D. Arnett. Type I supernovae. I - Analytic solutions for the early part of the light curve. , 253:785–797, February 1982. doi: 10.1086/159681.

J. Barnes and D. Kasen. Effect of a High Opacity on the Light Curves of Radioactively Powered Transients from Compact Object Mergers. , 775:18, September 2013. doi: 10.1088/0004-637X/775/1/18.

J. Barnes, D. Kasen, M.-R. Wu, and G. Martínez-Pinedo. Radioactivity and Thermalization in the Ejecta of Compact Object Mergers and Their Impact on Kilonova Light Curves. , 829:110, October 2016. doi: 10.3847/0004-637X/829/2/110.

E. Berger, W. Fong, and R. Chornock. An r-process Kilonova Associated with the Short-hard GRB 130603B. , 774:L23, September 2013. doi: 10.1088/2041-8205/774/2/L23.

W. Fong, E. Berger, R. Margutti, and B. A. Zauderer. A Decade of Short-duration Gamma-Ray Burst Broadband Afterglows: Energetics, Circumburst Densities, and Jet Opening Angles. , 815:102, December 2015. doi: 10.1088/0004-637X/815/2/102.

C. J. Fontes, C. L. Fryer, A. L. Hungerford, R. T. Wollaeger, S. Rosswog, and E. Berger. A line-smeared treatment of opacities for the spectra and light curves from macronovae. *ArXiv e-prints*, February 2017.

K. Hotokezaka, K. Kyutoku, Y.-i. Sekiguchi, and M. Shibata. Measurability of the tidal deformability by gravitational waves from coalescing binary neutron stars. , 93(6):064082, March 2016. doi: 10.1103/PhysRevD.93.064082.

Z.-P. Jin, K. Hotokezaka, X. Li, M. Tanaka, P. D'Avanzo, Y.-Z. Fan, S. Covino, D.-M. Wei, and T. Piran. The Macronova in GRB 050709 and the GRB-macronova connection. *Nature Communications*, 7:12898, September 2016. doi: 10.1038/ncomms12898.

D. Kasen, R. Fernández, and B. D. Metzger. Kilonova light curves from the disc wind outflows of compact object mergers. , 450:1777–1786, June 2015. doi: 10.1093/mnras/stv721.

O. Korobkin, S. Rosswog, A. Arcones, and C. Winteler. On the astrophysical robustness of the neutron star merger r-process. , 426:1940–1949, November 2012. doi: 10.1111/j.1365-2966.2012.21859.x.

T. M. Koshut, W. S. Paciesas, C. Kouveliotou, J. van Paradijs, G. N. Pendleton, G. J. Fishman, and C. A. Meegan. T_{90} as a Measurment of the Duration of GRBs. In *American Astronomical Society Meeting Abstracts #186*, volume 27 of *Bulletin of the American Astronomical Society*, page 886, May 1995.

L.-X. Li and B. Paczyński. Transient Events from Neutron Star Mergers. , 507: L59–L62, November 1998. doi: 10.1086/311680.

B. D. Metzger, G. Martínez-Pinedo, S. Darbha, E. Quataert, A. Arcones, D. Kasen, R. Thomas, P. Nugent, I. V. Panov, and N. T. Zinner. Electromagnetic counterparts of compact object mergers powered by the radioactive decay of r-process nuclei. , 406:2650–2662, August 2010. doi: 10.1111/j.1365-2966.2010.16864.x.

M. Nicholl, J. Guillochon, and E. Berger. The magnetar model for Type I superluminous supernovae I: Bayesian analysis of the full multicolour light curve sample with MOSFiT. *ArXiv e-prints*, June 2017.

F. Pannarale and F. Ohme. Prospects for Joint Gravitational-wave and Electromagnetic Observations of Neutron-star-Black-hole Coalescing Binaries. , 791:L7, August 2014. doi: 10.1088/2041-8205/791/1/L7.

L. F. Roberts, D. Kasen, W. H. Lee, and E. Ramirez-Ruiz. Electromagnetic Transients Powered by Nuclear Decay in the Tidal Tails of Coalescing Compact Binaries. , 736:L21, July 2011. doi: 10.1088/2041-8205/736/1/L21.

S. Rosswog, U. Feindt, O. Korobkin, M.-R. Wu, J. Sollerman, A. Goobar, and G. Martinez-Pinedo. Detectability of compact binary merger macronovae. *Classical and Quantum Gravity*, 34(10):104001, May 2017. doi: 10.1088/1361-6382/aa68a9.

R. Sari, T. Piran, and R. Narayan. Spectra and Light Curves of Gamma-Ray Burst Afterglows. , 497:L17–L20, April 1998. doi: 10.1086/311269.

V. V. Sobolev. *Moving envelopes of stars*. 1960.

N. R. Tanvir, A. J. Levan, A. S. Fruchter, J. Hjorth, R. A. Hounsell, K. Wiersema, and R. L. Tunnicliffe. A 'kilonova' associated with the short-duration γ-ray burst GRB 130603B. , 500:547–549, August 2013. doi: 10.1038/nature12505.

The LIGO Scientific Collaboration, the Virgo Collaboration, R. Abbott, T. D. Abbott, F. Acernese, K. Ackley, C. Adams, T. Adams, P. Addesso, R. X. Adhikari, and et al. GW170814: A three-detector observation of gravitational waves from a binary black hole coalescence. *ArXiv e-prints*, September 2017.

R. T. Wollaeger, O. Korobkin, C. J. Fontes, S. K. Rosswog, W. P. Even, C. L. Fryer, J. Sollerman, A. L. Hungerford, D. R. van Rossum, and A. B. Wollaber. Impact of ejecta morphology and composition on the electromagnetic signatures of neutron star mergers. *ArXiv e-prints*, May 2017.

B. Yang, Z.-P. Jin, X. Li, S. Covino, X.-Z. Zheng, K. Hotokezaka, Y.-Z. Fan, T. Piran, and D.-M. Wei. A possible macronova in the late afterglow of the long-short burst GRB 060614. *Nature Communications*, 6:7323, June 2015. doi: 10.1038/ncomms8323.

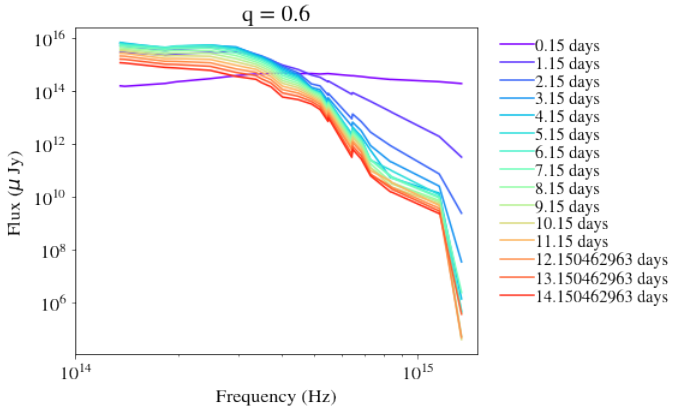

(a)

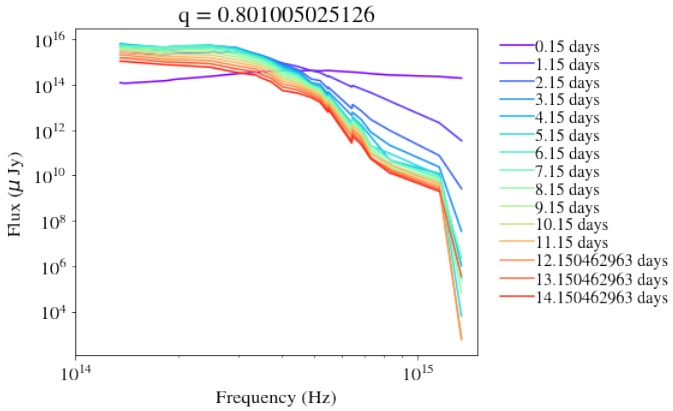

(b)

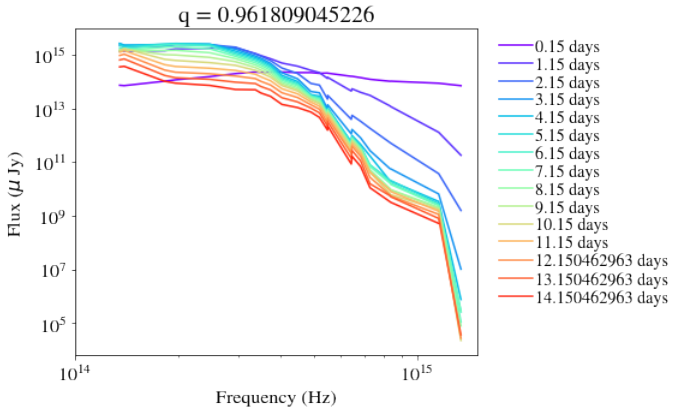

(c)

Figure 7: Three different sets of macronova spectra obtained from our interpolation of Barnes & Kasen models for three different values of mass ratio.

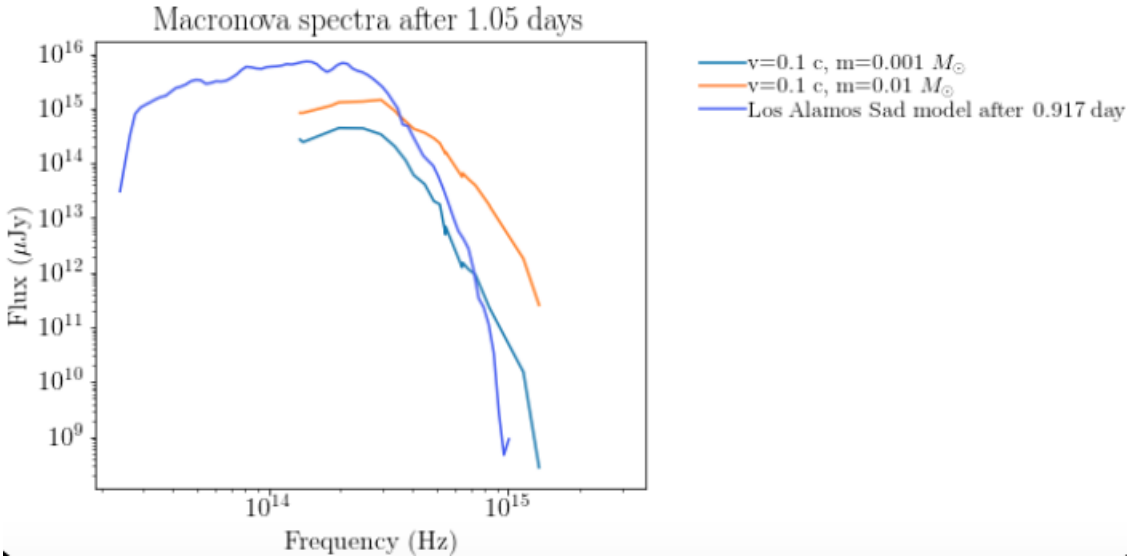

Figure 8: Comparison between bp_CaFN_lv_l and bp_CaFN_lv_m models with the SAd model from Wollaeger et al. [2017].

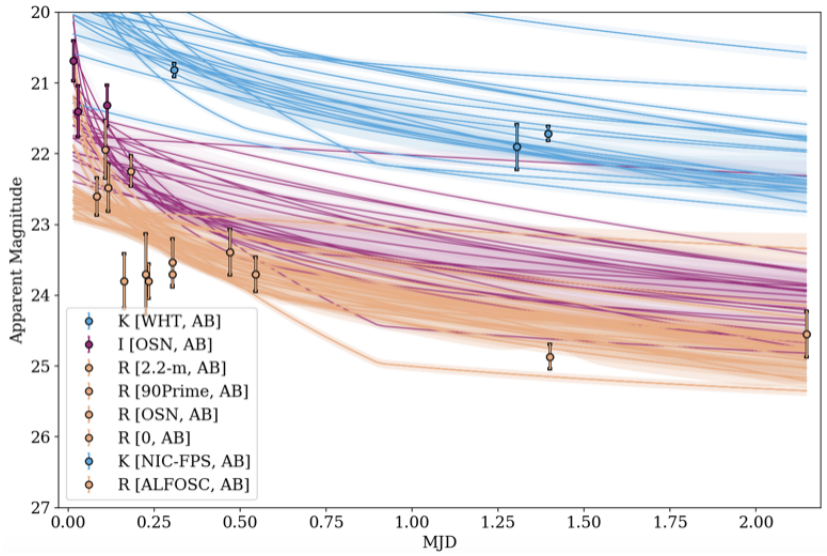

Figure 9: A preliminary fit of GRB 060121 with an afterglow model using the code MOSFiT. Different colors denotes K, I and R spectral bands. The dots in orange excluded from the fit are datas obtained by instruments whose filters are not included into MOSFiT.